






Time-varying Operating Regions of End-users and Feeders in Low-voltage Distribution Networks

Gayan Lankeshwara , *Student Member, IEEE*, Rahul Sharma , *Senior Member, IEEE*,
Ruifeng Yan , *Member, IEEE*, Tapan K. Saha , *Fellow, IEEE*, and Jovica V. Milanović , *Fellow, IEEE*

Abstract—Dynamic operating envelopes (DOEs) are promising to cater for the strong uptake of distributed energy resources (DERs) in low-voltage (LV) distribution networks while ensuring secure network operation. Under the current framework, DOEs only specify active-reactive power set-points at households' point of connection (POC). In this regard, DOEs do not provide information on the feasible operating region (FOR) of end-users, which is helpful for an aggregator's market decisions. This paper proposes a near real-time approach to determine DOEs that specify the FOR at end-users' POC in an LV distribution network. First, Latin hypercube sampling (LHS)-based load flow studies are performed to identify feasible pairs of P-Q injections at the POC that would not breach voltage limits. Secondly, the *convex hull* of feasible pairs is constructed to obtain household DOEs. Finally, a feeder-level time-varying envelope that represents the aggregate flexibility of downstream nodes of the network is calculated. A comprehensive analysis on a real Australian LV distribution network using realistic data suggests that the proposed approach is scalable and encourages active power exports beyond current industry practice. Moreover, the framework ensures privacy and separation between the distribution network service provider (DNSP) and the aggregator aligned with the existing policy and regulatory frameworks.

Index Terms—Dynamic operating envelopes (DOEs), feasible operating region (FOR), load flow analysis, computational geometry, voltage limits, probability, distributed energy resources

NOMENCLATURE

Sets

\mathcal{H}	Houses indexed by h ; $\mathcal{H} = \{1, 2, \dots, H\}$
\mathcal{N}	Three-phase P-Q buses indexed by i, k
Φ	Phases indexed by s, γ ; $\Phi = \{1, 2, 3\}$
\mathcal{T}	Time period indexed by t
\mathbb{R}^2	All ordered pairs of real numbers

Parameters

\bar{v}, \underline{v}	Upper and lower limits of voltages
φ_L^h	Power factor of uncontrollable load at house h
$G_{ik}^{s\gamma}$	conductance between phase s and γ for the line connecting bus i and k
$B_{ik}^{s\gamma}$	susceptance between phase s and γ for the line connecting bus i and k

Variables

$V_{i,t}^s$	Complex voltage of phase s in bus i at time t
-------------	---

Gayan Lankeshwara, Rahul Sharma, Ruifeng Yan and Tapan K. Saha are with the School of Information Technology and Electrical Engineering, The University of Queensland, Brisbane, QLD 4072, Australia (email: g.lankeshwara@uqconnect.edu.au, rahul.sharma@uq.edu.au, ruifeng@itee.uq.edu.au and saha@itee.uq.edu.au), Jovica V. Milanović is with the Department of Electrical & Electronic Engineering, The University of Manchester, United Kingdom (email: jovica.milanovic@manchester.ac.uk).

$P_{inj,t}^h, Q_{inj,t}^h$	Active and reactive power injection at the POC of house h at time t
$\tilde{P}_{L,t}^h, \tilde{Q}_{L,t}^h$	Active and reactive power consumption of uncontrollable loads of house h at time t
$P_{PV,t}^h, Q_{PV,t}^h$	Active and reactive power set-point of rooftop PV in house h at time t
$\tilde{P}_{PV,t}^h$	Available active power generation of house h at time t
$\bar{P}_{inj,t}^h, \bar{Q}_{inj,t}^h$	Maximum limits of active and reactive power injection at the POC of house h at time t
$\underline{P}_{inj,t}^h, \underline{Q}_{inj,t}^h$	Minimum limits of active and reactive power injection at the POC of house h at time t
$P_{inj,t}^{h,\omega}, Q_{inj,t}^{h,\omega}$	Active and reactive power injection at the POC of house h under scenario ω at time t

Envelopes related notation

\mathfrak{B}_t^h	Bounding box in the P-Q space for house h at time t
\mathcal{B}_t^h	Feasible region of operation in the P-Q space for the POC of house h at time t
\mathcal{B}^h	Time-invariant envelope in the P-Q space outlining the overall FOR at POC for house h for the forward horizon
\mathcal{A}_t	Aggregate envelope of downstream nodes at time t
\mathcal{A}	Aggregate time-invariant envelope outlining the overall FOR for the forward horizon

Other operators

$\Re(\cdot)$	Real part of a complex number
$\Im(\cdot)$	Imaginary part of a complex number
$\text{conv}(\cdot)$	Convex hull operator
\oplus	Minkowski sum

I. INTRODUCTION

The rapid proliferation of consumer-owned distributed energy resources (DERs) in low-voltage (LV) networks and their participation in electricity markets has created complex technical challenges for distribution network service providers (DNSPs) to manage the secure operation of the grid. The conventional approach to mitigate these challenges is to impose static import/export limits and curtail excess power beyond the pre-defined limit. For instance, Energex, the DNSPs in Queensland, Australia, adopts 5 kW export limits (single-phase) at the connection point for small-scale embedded generation [1]. Nonetheless, this approach leads to under-utilisation of consumer-owned DERs as static limits are determined by considering worst-case loading and generation scenarios [2].

Dynamic operating envelopes (DOEs) are promising for efficiently utilising the existing electricity infrastructure whilst respecting network constraints. For instance, Energex is currently in the process of adopting dynamic customer connections to facilitate the continued uptake of DERs and to maximise the utilisation of existing network assets [1]. According to [2], DOEs are defined as “operating envelopes that vary import and export limits over time and location based on the available capacity of the local network or power system as a whole”. Aligned with this definition, DOEs can be implemented at device level or the point of connection (POC) of an end-user [3].

Considering the state-of-the-art literature, DOE allocation mechanisms can be mainly categorised under three groups: 1) optimal power flow (OPF)-based allocation; 2) allocation based on unbalanced power flows; 3) allocation based on network sensitivities.

In OPF-based approaches, an optimisation problem is formulated with the design objective reflecting the operation of the central utility, e.g., minimising losses for the DNSP, maximising social welfare for the distributed energy resources aggregator (DERA); the constraints capture power balance, network statutory limits and the operational limits of consumer-owned DERs. The solution determines household DOEs at each time instant. For instance, the authors in [4] propose two architectures for OPF-based DOE calculations depending on the time horizon of interest and the availability of data. In the near real-time approach, operating envelopes are calculated for the upcoming interval, e.g., every 5-mins, 15-mins. In the in-advance approach, operating envelopes are calculated for all intervals on the horizon to be considered (e.g., next 6-hours, 24-hours). The allocation of DOEs is studied for three objective functions such as maximising total exports, fair allocation with each customer adopting the same export limit and weighted allocation of exports [5]. Moreover, the algorithm separately determines import and export limits at the POC of end-users. Nonetheless, the calculated DOEs only correspond to active power limits.

In [6], an unbalanced three-phase AC-OPF problem is solved at each time step to assign DOEs for the DERA to participate in day-ahead markets. However, the adoption of DOEs is only permitted to household active power export limits and neglect the impact of household import limits and reactive power in managing secure network operation. In [7], an AC-OPF problem is solved to assign dynamic operating limits only if the end-user intended operation compromises voltage limits of the distribution network. However, limiting active power injections at the POC is only considered, and there is no guarantee that end-user data privacy [8] is preserved as they are required to share forecasts of household load and generation with the DNSP.

Ref. [9] proposes a bi-level framework for the computation of operating envelopes using an AC-OPF approach. In this scheme, the DNSP calculates DOEs at the upper-level for the day-ahead using forecasts of household load and generation. In the lower level, end-users coordinate DERs in real-time for household energy management based on DOEs determined by the DNSP. However, only active power export limits are

considered and there is no guarantee that the approach is applicable for the market participation of DERs via a DERA. Moreover, the analysis is based on a single-phase equivalent of a three-phase network, and is not realistic considering practical LV distribution networks. The authors in [10] have proposed an end-user privacy-preserving, distributed control approach based on AC-OPF to allocate network-secure envelopes for end-users to participate in electricity markets without breaching technical limits of the network. Furthermore, a Q-P controller which facilitates end-user reactive power is also proposed.

With regard to unbalanced power flow based approaches, the authors in [3] highlight the importance of capturing AC physics of the electricity grid to determined DOEs with reference to physical and operational constraints. Thereby, a four-step process is proposed to publish DOEs for end-users. The first step is to determine uncontrollable power flows due to uncontrollable demand and generation, and determining the available hosting capacity, i.e., the amount of DERs that can be installed and operated in a distribution network without breaching technical and operational limits. The second step is to identify the connection points that need to use the available hosting capacity. The third step is choosing an allocation method (as discussed in [5]) and calculating the capacity allocated to each connection point. Finally, the DOEs are published for each connection point. Ref. [11] proposes a novel approach for calculating active and reactive power operating envelopes using a two-stage algorithm. The calculated envelopes correspond to the intersection of voltage safe operating region and current safe operating region in the P-Q plane. Nonetheless, the main focus is on DOEs for network-safe household energy management in LV distribution networks, and therefore, fails to address how DOEs can be adopted when a cohort of DERs participate in market services via a DERA. The authors in [12] analyse the impact of nodal voltage sensitivities in unbalanced LV distribution networks on the effectiveness of DOEs. A bijection algorithm is adopted to calculate DOEs which correspond to active power exports and imports. However, it is assumed that all customers are subject to the same DOE at a certain time instant.

In sensitivity-based approaches [13], [14], sensitivities of network parameters, e.g., voltages and currents, with respect to active and reactive power are calculated using different techniques—regression, Jacobian method, perturb-and-observe method. After that, the sensitivity factors are used to determine power injections at each POC such that network operating limits are preserved. For example, the authors in [14] have proposed a coordinated scheme where the DNSP calculates network sensitivities using a linear regression technique and sends to the DERA for its day-ahead scheduling and real-time operation.

In the existing literature [2], [4], [9], [10], [15], the notion of DOEs is aligned with active and reactive power dispatch set-points for DER devices or at the POC of end-users. However, these set-points calculated based on diverse design objectives do not necessarily represent an envelope; instead gives a single feasible point in the P-Q space of a DER device or at the POC of an end-user for which the network statutory limits are

not compromised. Moreover, explicit set-points are insufficient to provide information on flexibility at the POC of an end-user at a particular instant. Nonetheless, suppose adequate information is available to evaluate an envelope encapsulating the FOR in the P-Q plane for a household at a specific time step. In that case, it will be helpful for the DERA in its electricity market decisions [16].

Although there is a large volume of published work on managing electric flexibility from DERs [16]–[20], most studies have predominantly focussed on determining aggregate flexibility at the transmission-distribution interface for ancillary service provisions. For example, the authors in [18] have adopted *nodal operating envelopes*—obtained using individual P-Q capability curves of grid-connected PV and battery storage—to model DER flexibility in medium-voltage (MV) networks. Ref. [19] proposes time-dependent FOR and utilises a probabilistic approach to determine the aggregate flexibility of an active distribution network to provide ancillary services while regulating transmission flows. In [20], the epsilon-constrained method is adopted to generate the boundary of the feasibility region at the transmission-distribution interface; thereafter, a multi-period OPF problem is solved to obtain time-varying feasibility envelopes at the interface. Unlike aforementioned studies, the DNSP has no knowledge of P-Q capability curves at the POC of end-users in LV networks due to: data privacy concerns [8], aggregation of multiple DER devices at the POC coordinated via a Home Energy Management System (HEMS). Hence, the approaches mentioned above cannot be adopted to determine household-level operating envelopes that specify FOR without breaching the technical limits of the network and feeder-level DOEs in LV distribution networks.

Aligned with the ‘hybrid model’ [21] (widely accepted framework for integrating DERs for market participation in Australia), DNSP is responsible for creating DOEs that specify operational limits for DERs while delivering wholesale and/or local network support services. On the other hand, the DERA is responsible for the aggregation of consumer-owned DERs and the delivery of service while accommodating DOEs [22]. In this regard, [2], [3] highlight the importance of adopting DOEs at the customer connection point (irrespective of number of configurations of devices behind the connection) during the DOE roll-out process. Therefore, the most effective approach for adopting DOEs in a realistic setting would be: DNSP calculating DOEs at household connection points based on available network information, and thereafter, sharing DOEs with the DERA to be utilised in the market participation process. However, only a handful of existing studies [6], [7], [15], [23] have explicitly identified DNSP and DERA as two different stakeholders in the overall implementation. Therefore, systematic coordination between the DNSP and the DERA in compliance with existing policy and regulatory framework is crucial for the practical implementation of DOEs enabling end-user participation in electricity markets [2], [24]. A summary of the existing work on network-aware control of DERs is given in Table I.

TABLE I
A COMPARISON OF THE EXISTING APPROACHES ON NETWORK-AWARE MARKET PARTICIPATION OF DERs

Ref.	Envelopes represent flexibility	Reactive power contribution	End-user privacy	DNSP-DERA coordination
[6]	×	×	×	✓
[7]	×	×	×	✓
[9]	×	×	✓	✓
[10]	×	✓	✓	×
[11]	×	✓	✓	×
[12]	×	×	×	×
[15]	×	×	✓	✓
[18]	✓	✓	N/A	N/A
[19]	✓	✓	N/A	N/A
[20]	✓	✓	N/A	N/A
[23]	×	✓	×	✓
[25]	×	✓	✓	×
[26]	×	×	×	×
<i>proposed</i>	✓	✓	✓	✓

– N/A represents not-applicable.

Main contributions

The main contributions of this work can be summarised as follows:

- A near real-time approach is proposed for the DNSP to determine operating envelopes that outline feasible operating regions (FORs) in the P-Q plane without breaching network voltage limits. Unlike existing approaches where OPF-based explicit set-points are adopted as operating envelopes, household P-Q operating regions determined in this work provide information on end-user flexibility which is useful for DERA’s decisions in electricity markets.
- The aggregate time-varying flexibility of an LV distribution network is determined by accommodating individual household operating envelopes. Furthermore, household-level and feeder-level time invariant envelopes that benefit the DERA in day-ahead scheduling in electricity markets are constructed.
- The privacy and separation between the DNSP, DERA and the end-user are ensured with minimum data sharing requirements. This is achieved by end-users only sharing minimum and maximum power injection limits with the DNSP. Thereafter, DOEs are determined by the DNSP and then shared with the DERA while preserving network-specific information.

II. PROPOSED METHODOLOGY

The main objective of this work is to propose an approach for the DNSP to determine DOEs that specify the FOR at the POC of each end-user in real-time. A block diagram summarising the steps involved in the overall approach is given in Fig. 1. According to the figure, the calculation of DOEs can be discussed in two stages: 1) household problem which determines the bounds of operation of each household; 2) DNSP problem which adopts LHS method followed by

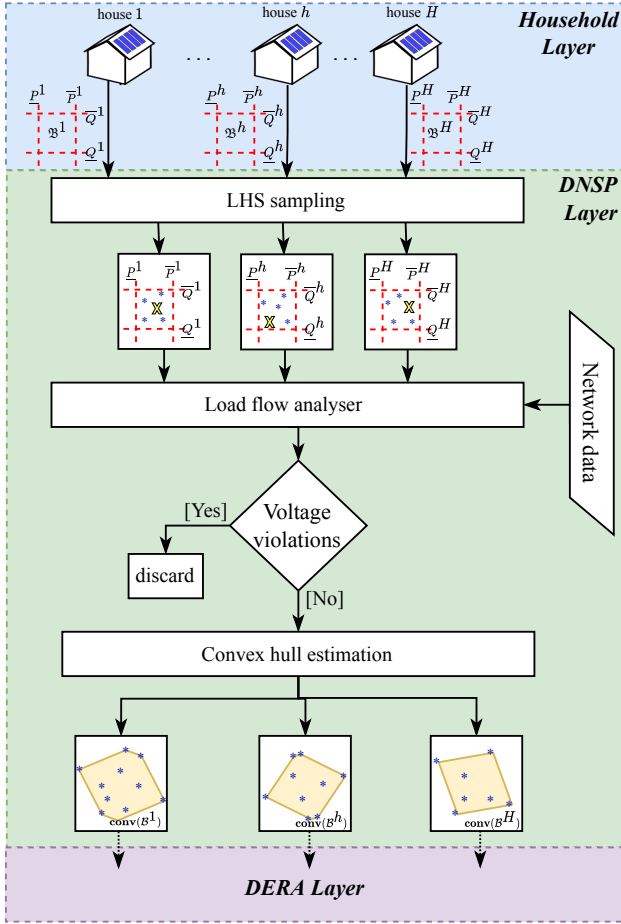


Fig. 1. A flow diagram showing the overall process of determining household DOEs at each sampling instant

a convex hull approximation to determining DOEs for each household. This is discussed in detail in the following sections.

A. Household problem

As the first step, each household is required to estimate the minimum and maximum limits of active and reactive power injections at each time instant based on near real-time measurements of consumption and generation.

Let $\mathcal{H} := \{1, 2, \dots, H\}$ be the set of houses indexed by h and $\mathcal{T} := \{t_0, t_0 + 1, \dots, t_0 + T\}$ be the set of time periods indexed by t . Considering rooftop PV generation to be the household controllable DER device, the active and reactive power injection at the POC of household $h \in \mathcal{H}$ at time $t \in \mathcal{T}$ can be expressed as:

$$P_{inj,t}^h = P_{PV,t}^h - \tilde{P}_{L,t}^h \quad (1)$$

$$Q_{inj,t}^h = Q_{PV,t}^h - \tilde{Q}_{L,t}^h \quad (2)$$

where the notations are included in the Nomenclature section. To this end, a positive power injection represents exporting power to the grid whereas a negative injection represents absorbing power from the grid at the POC.

Aligned with the state-of-the-art literature [27], [28] and inverter standards [29], active and reactive power control under a minimum power factor is considered for the operation of the rooftop PV inverter. This can be mathematically expressed as:

$$0 \leq P_{PV,t}^h \leq \tilde{P}_{PV,t}^h \quad (3)$$

$$-P_{PV,t}^h \tan(\cos^{-1}(\varphi_{PV}^h)) \leq Q_{PV,t}^h \quad (4)$$

$$\leq P_{PV,t}^h \tan(\cos^{-1}(\varphi_{PV}^h))$$

For uncontrollable load, the relationship between active and reactive power can be expressed as:

$$\tilde{Q}_{L,t}^h = \tilde{P}_{L,t}^h \tan(\cos^{-1}(\varphi_L^h)), \quad t \in \mathcal{T} \quad (5)$$

where the notation is given in the Nomenclature section. Following this, the minimum and maximum limits of active and reactive power injection at the POC of household h at time $t \in \mathcal{T}$ can be algebraically calculated as:

$$\underline{P}_{inj,t}^h = \min(P_{inj,t}^h) \quad \text{s.t. (1) - (5)} \quad (6)$$

$$\overline{P}_{inj,t}^h = \max(P_{inj,t}^h) \quad \text{s.t. (1) - (5)} \quad (7)$$

$$\underline{Q}_{inj,t}^h = \min(Q_{inj,t}^h) \quad \text{s.t. (1) - (5)} \quad (8)$$

$$\overline{Q}_{inj,t}^h = \max(Q_{inj,t}^h) \quad \text{s.t. (1) - (5)} \quad (9)$$

To explain this, since household load is $\tilde{P}_{L,t}^h$ uncontrollable, $\underline{P}_{inj,t}^h$ in (6) can be estimated by setting the controllable PV generation $P_{PV,t}^h$ at its minimum which is zero, as given in (3). On the other hand, $\overline{P}_{inj,t}^h$ in (7) can be calculated by setting $P_{PV,t}^h$ at its maximum value which is $\tilde{P}_{PV,t}^h$. Similarly, $\underline{Q}_{inj,t}^h$ and $\overline{Q}_{inj,t}^h$ can also be calculated by taking into account (1)-(5).

Once household h calculates $[\underline{P}_{inj,t}^h, \overline{P}_{inj,t}^h, \underline{Q}_{inj,t}^h, \overline{Q}_{inj,t}^h]$ at time $t \in \mathcal{T}$, then it estimates the region of operation in the P-Q space ($\subset \mathbb{R}^2$) at the POC via a bounding box approximation. For household h , the bounding box that captures the operating region at the POC at time $t \in \mathcal{T}$ can be expressed as:

$$\mathfrak{B}_t^h := \left\{ (P_{inj,t}^h, Q_{inj,t}^h) \left| \begin{array}{l} \underline{P}_{inj,t}^h \leq P_{inj,t}^h \leq \overline{P}_{inj,t}^h \\ \underline{Q}_{inj,t}^h \leq Q_{inj,t}^h \leq \overline{Q}_{inj,t}^h \end{array} \right. \right\} \quad (10)$$

where $(P_{inj,t}^h, Q_{inj,t}^h)$ pair corresponds to active and reactive power at the POC of household h at time t . Afterwards, each household sends the information on \mathfrak{B}_t^h at time $t \in \mathcal{T}$ to the DNSP via the existing bi-directional communication infrastructure which is assumed to be fail-proof.

It is important to highlight that \mathfrak{B}_t^h in (10) generally overestimates the feasible region of operation at the POC of household h . In other words, for any household scheduling problem where the solution space is limited to $(P_{inj,t}^h, Q_{inj,t}^h) \in \mathfrak{B}_t^h \subset \mathbb{R}^2$ for $h \in \mathcal{H}$ at time t , there is no guarantee that subsequent power flows in the network would regulate voltages within technical limits.

Nevertheless, each household can calculate power injection limits given by (6)-(9) and the operating region described by (10) locally via existing HEMS [30] infrastructure based on near real-time measurements of load and generation. Thereafter, each household shares minimal information—only

the operating envelope given by (10)—with the DNSP. This alleviates the need for households to share consumption and generation profiles with the DNSP at each time instant. Even if the DNSP is aware of household PV inverter ratings (via the DER register [31]), by only sharing an envelope describing the operating region given by (10), households are not required to share any information on controllable loads and battery energy storage systems in their premises that would provide demand response services. Thus, it is guaranteed that the proposed approach preserves end-user data privacy.

B. DNSP problem

As discussed in section II-A, the envelopes determined at household-level are network-agnostic and the operation would compromise voltage statutory limits of the network. In other words, the envelopes do not capture the FOR of each household at a certain time step. To this end, the DNSP utilises a systematic approach: 1) determining DOEs in real-time for each household that encapsulates the FOR; 2) determining a feeder-level aggregate envelope; 3) estimating the overall FOR of households over a period of time based on forecasts of household measurements. The overall process is described in the following sections.

1) Determining DOEs at the POC of households

After each household shares information on its envelope at time t , the DNSP utilises a probabilistic load flow technique to determine feasible P-Q injection pairs $(P_{inj,t}^h, Q_{inj,t}^h) \in \mathfrak{B}_t^h$ for all h that would not breach voltage limits at any node of the network. To this end, samples of P-Q injections are generated from their own envelope at a certain time step using the Latin hypercube sampling (LHS) method for each household. The motivation behind the LHS method is to avoid the significant computational burden associated with the generation of extensive random samples under the traditional Monte Carlo (MC) sampling method. Instead, the LHS method ensures that the whole search space is evenly sampled, thus, improving the search space coverage [32]. Moreover, random sampling methods adequate to determine FOR in comparatively small electric grids [33]. An illustration of random P-Q injection pairs for a certain household generated using MC method and the LHS method is given in Fig. 2.

Let N_s be the number of samples of $(P_{inj,t}^h, Q_{inj,t}^h) \in \mathfrak{B}_t^h$ pairs generated for all $h \in \mathcal{H}$ at time $t \in \mathcal{T}$ under the LHS

method. In the next step, the DNSP randomly chooses a single pair of P-Q injections from the search space for each household and solves a three-phase power flow problem to check for voltage violations. The three-phase power flow equations for active power injection and reactive power injection can be expressed as:

$$P_{i,t}^s = \Re(V_{i,t}^s) \sum_{k \in \mathcal{N}} \sum_{\gamma \in \Phi} [G_{ik}^{s\gamma} \cdot \Re(V_{k,t}^s) - B_{ik}^{s\gamma} \cdot \Im(V_{k,t}^s)] + \Im(V_{i,t}^s) \sum_{k \in \mathcal{N}} \sum_{\gamma \in \Phi} [G_{ik}^{s\gamma} \cdot \Im(V_{k,t}^s) + B_{ik}^{s\gamma} \cdot \Re(V_{k,t}^s)]$$

$$i \in \mathcal{N}, s \in \Phi, t \in \mathcal{T} \quad (11)$$

$$Q_{i,t}^s = \Im(V_{i,t}^s) \sum_{k \in \mathcal{N}} \sum_{\gamma \in \Phi} [G_{ik}^{s\gamma} \cdot \Re(V_{k,t}^s) - B_{ik}^{s\gamma} \cdot \Im(V_{k,t}^s)] - \Re(V_{i,t}^s) \sum_{k \in \mathcal{N}} \sum_{\gamma \in \Phi} [G_{ik}^{s\gamma} \cdot \Im(V_{k,t}^s) + B_{ik}^{s\gamma} \cdot \Re(V_{k,t}^s)]$$

$$i \in \mathcal{N}, s \in \Phi, t \in \mathcal{T} \quad (12)$$

where $\Re(\cdot)$ and $\Im(\cdot)$ represents *real* and *imaginary* parts of a complex number, $G_{ik}^{s\gamma}$ is the conductance and $B_{ik}^{s\gamma}$ is the susceptance between phase s and γ for the line between bus i and k , $P_{i,t}^s$ and $Q_{i,t}^s$ represents active and reactive power injection at phase s in bus i at time t . Since each phase of a particular bus has a household connected to it, $P_{i,t}^s$ and $Q_{i,t}^s$ can be equivalently represented as $P_{inj,t}^h$ and $Q_{inj,t}^h$.

It should be noted that this approach assumes DNSP has full information on the configuration and parameters of the network, and measurement data to perform load flow studies. In the absence of full network operational visibility, distribution system state estimation techniques discussed in [34], [35] can be utilised to determine load flows in the distribution network.

If the resulting three-phase load flow does not result in a breach of voltage limits for any node $i \in \mathcal{N}$, the corresponding P-Q injection pair for each house is considered feasible. On the other hand, if the resulting three-phase load flow compromises voltage limits at any node $i \in \mathcal{N}$ in the network, the corresponding P-Q injection pair is discarded from the solution space for each household. Likewise, the DNSP performs N_s three-phase load flow scenarios at a certain time step to determine feasible pairs of P-Q injections at the POC of each household. Following this, the FOR at the POC of household h at time $t \in \mathcal{T}$ given by $\mathcal{B}_t^h \subseteq \mathfrak{B}_t^h \subset \mathbb{R}^2$ can be mathematically expressed as:

$$\mathcal{B}_t^h := \left\{ \left(P_{inj,t}^{h,\omega}, Q_{inj,t}^{h,\omega} \right) \left| \begin{array}{l} \underline{v} \leq |V_{i,t}^s| \leq \bar{v} \\ (11), (12) \\ \omega \in \{1, 2, \dots, N_s\} \\ \forall i \in \mathcal{N}, s \in \Phi \end{array} \right. \right\} \quad (13)$$

where ω is the index of LHS sampling scenarios.

Compared to a set of P-Q injection pairs representing explicit set-points that a POC can attain, determining an operating envelope, i.e., a closed and bounded set, that encapsulates the FOR at the POC is beneficial for the DERA in its decision-making process in electricity markets. Considering

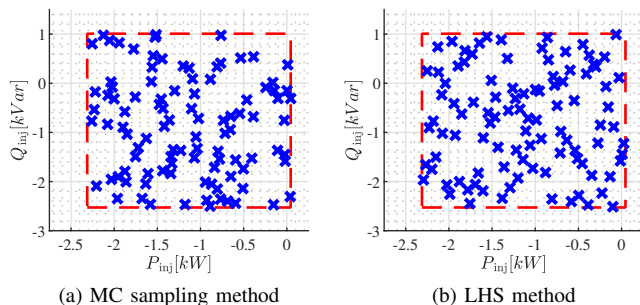


Fig. 2. Comparison of MC sampling and LHS within the region of operation for a household at a certain sampling instant ($N_s = 100$)

this, the operating envelope at the POC of house h at time t is obtained by constructing the *convex hull* [36] of all feasible pairs of $(P_{\text{inj},t}^h, Q_{\text{inj},t}^h) \in \mathcal{B}_t^h$ in the P-Q space. Since $(P_{\text{inj},t}^h, Q_{\text{inj},t}^h) \subset \mathbb{R}^2$ for $h \in \mathcal{H}$ at time t , the representation of *convex hull* simplifies to a convex polygon. Therefore, considering the *half-space representation* of the convex polygon [36], the operating envelope for household h at time t can be mathematically expressed as:

$$\mathbf{conv}(\mathcal{B}_t^h) := \left\{ (P_{\text{inj},t}^h, Q_{\text{inj},t}^h) \mid \mathbf{A} \cdot [P_{\text{inj},t}^h, Q_{\text{inj},t}^h]^T \leq \mathbf{b} \right\} \quad (14)$$

where $\mathbf{A} \in \mathbb{R}^{m \times 2}$, $\mathbf{b} \in \mathbb{R}^m$ and $m \leq N_s$. In addition to that, (14) can be easily calculated in time $\mathcal{O}(n \log n)$ with *Multi-Parametric Toolbox (MPT3)* [37].

On the other hand, the number of LHS samples required to accurately represent the search space and the number of three-phase load flow scenarios performed to determine feasible P-Q injection pairs for each household—both governed by N_s in this work—can be estimated as follows.

Let system state at a certain sampling instant be $S = [X_1, \dots, X_H]$ where X_h corresponds to a random pair of $(P_{\text{inj},t}^h, Q_{\text{inj},t}^h)$ obtained from the LHS space of household h and the random output of the system $f(S) = [Y_1, \dots, Y_{\mathcal{N}}]$ be the bus voltages following a three-phase load flow based on input states. The expected value of random output (i.e., voltages) is given by:

$$\mathbb{E}[f(S)] = \frac{1}{N_s} \sum_{\omega=1}^{N_s} f(S_\omega) \quad (15)$$

where S_ω is the ω -th sampled system state and $f(S_\omega)$ is the desired random output variable for ω -th sampled system state.

The variance of the expectation of desired random output is given by,

$$\text{Var}[\mathbb{E}[f(S)]] = \frac{\text{Var}[f(S)]}{N_s} \quad (16)$$

where $\text{Var}[f(S)]$ is the variance of $f(S)$ and obtained as:

$$\text{Var}[f(S)] = \frac{1}{N_s - 1} \sum_{\omega=1}^{N_s} (f(S_\omega) - \mathbb{E}[f(S)])^2 \quad (17)$$

Thereafter, the variance coefficient β can be estimated as:

$$\beta = \frac{\sqrt{\text{Var}[\mathbb{E}[f(S)]]}}{\mathbb{E}[f(S)]} \quad (18)$$

If ϵ is the threshold parameter (depends on the confidence interval) [32], Algorithm 1 can be used to estimate N_s .

Algorithm 1: Stopping criteria for the number of LHS samples

```

1 initialise  $N_s = 2$ ;
2 do
3   Calculate  $\beta_i$  for  $i \in \mathcal{N}$  using (15)-(18);
4   Estimate  $\beta_{\max}$  from  $\beta_i$  for  $i \in \mathcal{N}$ ;
5    $N_s = N_s + 1$ 
6 while  $\beta_{\max} > \epsilon$ ;

```

Once the DNSP calculates household operating envelopes for all $h \in \mathcal{H}$ at a certain time step, the information is passed to the DERA.

Unlike the conventional approach where the DNSP or the DERA calculates explicit operating set-points using OPF [10], [15], [38], time-varying household operating envelopes calculated in this method provide general information on the FOR, i.e., flexibility at the POC of each household at a certain time instant. Moreover, the DERA can utilise DOEs shared by the DNSP for real-time control of household devices to participate in wholesale and ancillary service markets. This could be achieved via a centralised or distributed control scheme [39] in which household operating envelopes are included as an additional constraint—which is convex—in the formulation. Hence, non-linear and non-convex formulations observed in typical OPF problems for the DERA can be avoided (the real-time market participation of the DERA based on assigned dynamic operating envelopes will be discussed in a future study). On the other hand, the DNSP is able to impose network constraints on the real-time market operation via dynamic operating envelopes without sharing network-specific information with the DERA.

The calculation of individual household DOEs employs a near-real time approach where household load and generation data for the upcoming interval (e.g., 5-mins, 15-mins) is considered. By considering a short time interval, for example, 5-mins, load and generation forecast uncertainties can be neglected in constructing household DOEs at a certain time instant.

2) Determining aggregate time-varying envelopes

In addition to time-varying envelopes that provide information on individual household flexibility, determining DOEs that aggregate the FOR of downstream nodes, i.e. households, will be beneficial for the DERA to assess the flexibility of a particular network and determine market decisions. To this end, the aggregate time-varying envelope of downstream nodes is evaluated by the *Minkowski sum* [36] of household DOEs.

Let $\mathbf{conv}(\mathcal{B}_t^1), \mathbf{conv}(\mathcal{B}_t^2), \dots, \mathbf{conv}(\mathcal{B}_t^H)$ be the set of DOEs of households at time $t \in \mathcal{T}$. Therefore, the aggregate envelope of downstream nodes (where households are connected) at time $t \in \mathcal{T}$ represented by \mathcal{A}_t can be obtained as:

$$\mathcal{A}_t = \mathbf{conv}(\mathcal{B}_t^1) \oplus \mathbf{conv}(\mathcal{B}_t^2) \oplus \dots \mathbf{conv}(\mathcal{B}_t^H) \quad (19)$$

where \oplus represents *Minkowski addition*.

3) Estimating operating envelopes for the offline operation

The household DOEs in section II-B1 and the aggregate operating envelope in section II-B2 are calculated in real-time based on near real-time measurements of household demand and generation. However, if household forecasts are available for a certain horizon, for example, 30-mins, 1-hour, 24-hours, such forecasts can be utilised to calculate household DOEs and aggregate operating envelopes offline. This information will be of practical importance for the DERA, especially in the planning stage. For instance, with 24-hours ahead forecasts of household load and generation data, the DNSP can estimate operating envelopes for the forward horizon and then utilise them to obtain an envelope for each household that outlines the overall FOR for that particular period. Thereafter, the

DNSP shares this 24-hour ahead operating envelope for each household with the DERA to utilise this information in its day-ahead scheduling operation.

Let $\text{conv}(\mathcal{B}_{t_0}^h), \text{conv}(\mathcal{B}_{t_0+1}^h), \dots, \text{conv}(\mathcal{B}_{t_0+T}^h)$ be the time-varying operating envelopes at the POC of household $h \in \mathcal{H}$ calculated as in section II-B1 for the period $[t_0, t_0+T]$, the envelope that outlines the overall FOR (\mathcal{B}^h) can be obtained as follows:

$$\mathcal{B}^h = \text{conv}(\text{conv}(\mathcal{B}_{t_0}^h), \text{conv}(\mathcal{B}_{t_0+1}^h), \dots, \text{conv}(\mathcal{B}_{t_0+T}^h)) \quad (20)$$

It should be noted here that \mathcal{B}^h for $h \in \mathcal{H}$ in (20) is constructed by obtaining the *convex hull* of time-varying operating envelopes. This is similar to obtaining an outer approximation of time-varying envelopes of a household. Since $(\mathcal{B}_{t_0+1}^h), \dots, \text{conv}(\mathcal{B}_{t_0+T}^h)$ represent $T+1$ number of convex sets such that $\mathcal{B}_t^h \in \mathbb{R}^2$ for $h \in \mathcal{H}$ and $t \in [t_0, t_0+T]$, the convex hull of $(\mathcal{B}_{t_0+1}^h), \dots, \text{conv}(\mathcal{B}_{t_0+T}^h)$ is also convex and can be calculated in time $\mathcal{O}(n \log n)$ [36]. Also, \mathcal{B}^h is time-invariant.

On the other hand, with household envelopes $\text{conv}(\mathcal{B}_t^h)$ for all h and $t \in [t_0, t_0+T]$, the aggregate time-varying envelopes \mathcal{A}_t for $t \in [t_0, t_0+T]$ can be calculated as in section II-B2. Thereafter, an envelope representing the overall FOR of downstream nodes of the network for the considered period can be obtained using an approach similar to the case where overall household FOR is determined.

Let $\mathcal{A}_{t_0}, \mathcal{A}_{t_0+1}, \dots, \mathcal{A}_{t_0+T}$ represent aggregate time-varying envelopes for the period $[t_0, t_0+T]$, then the envelope outlining the overall aggregate feasible region of operation of downstream nodes (\mathcal{A}^f) can be obtained as:

$$\mathcal{A}^f = \text{conv}(\mathcal{A}_{t_0}, \mathcal{A}_{t_0+1}, \dots, \mathcal{A}_{t_0+T}) \quad (21)$$

Similarly, \mathcal{A}^f in (21) is an outer convex approximation of time-varying aggregate envelopes and is time-invariant.

The aggregate time-invariant envelope \mathcal{A}^f quantifies the overall FOR for a particular period of time. On the other hand, considering day-ahead market participation, with such offline information from different LV feeder networks, the DERA is able to allocate power set-points to each upstream point of LV networks via an optimisation approach.

III. RESULTS AND DISCUSSION

The proposed approach is validated on a practical residential LV residential network in Queensland, Australia [40]. The single-line diagram of the network is shown in Fig. 3. Since network data is only available up to the pole-level, it is assumed that a single household is connected to each phase $s \in \Phi$ of all P-Q buses (bus ② to bus ③⑤). This results in a total of $34 \times 3 = 102$ customers.

It is assumed that each household $h \in \mathcal{H}$ is equipped with a rooftop PV inverter. The historical household load and generation profiles are obtained from the real-time monitoring platform associated with the pilot project conducted by the Centre for Energy Data Innovation at the University of Queensland (see [41] for more details). In this regard, 5-min sampled household load profiles of 12 residential customers and 5-min sampled rooftop PV generation profiles of

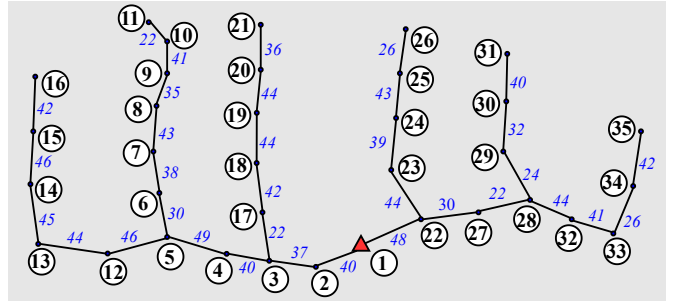


Fig. 3. The single line diagram of the LV residential network [40]; bus ① (red triangle) represents the LV distribution transformer; black dots (bus ② – bus ③⑤) represent P-Q buses (poles); a household is connected to each phase of each bus except ①; black lines represent overhead conductors; italicised numbers in blue represent pole-to-pole and transformer-to-pole distances in metres.

5 household customers are considered. Fig. 4 shows 5-min sampled normalised active power consumption profiles and PV generation profiles of the chosen set of households on 22-03-2020 for a period of 24-hours. The normalised profiles are randomly allocated among 102 households such that, for uncontrollable loads, the base consumption is assumed to vary between 2 to 6 kW with $\varphi_L^h = 0.95$ pf lagging (aligned with small customer connection standards of the DNSP [1]) for all h and for rooftop PV generation, inverter ratings are [3.0, 3.6, 4.0, 5.0, 6.0, 8.0] kWp with $\varphi_{PV}^h = 0.8 \forall h \in \mathcal{H}$ (lagging/leading) [42].

The overall algorithm is written in MATLAB on a desktop computer equipped with an Intel(R) Core i7 3.20 GHz CPU and 16 GB RAM. For three-phase load flow studies, the LV network in Fig. 3 is modelled in OpenDSS [43]. The voltage statutory limits are $\underline{v} = 0.95$ pu and $\bar{v} = 1.10$ pu [1]. The *convex hull* and *Minkowski sum* operations are performed in MPT3 [37]. Aligned with wholesale market operations of the National Electricity Market (NEM) [2], [44], the sampling size for calculating dynamic operating envelopes at the connection point of households (described in section II-B1) is chosen to be 5-mins.

As the first step, the number of samples in the LHS search space of each household (same as the number of load flow scenarios) is determined as described in Algorithm 1 in

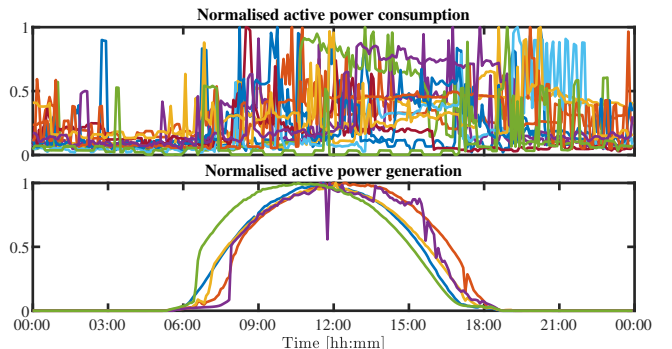
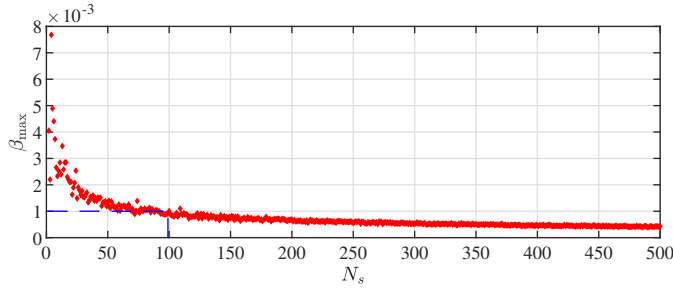


Fig. 4. Normalised profiles of active power consumption of loads and active power generation of rooftop PV for a period of 24-hours

Fig. 5. Determining N_s for LHS

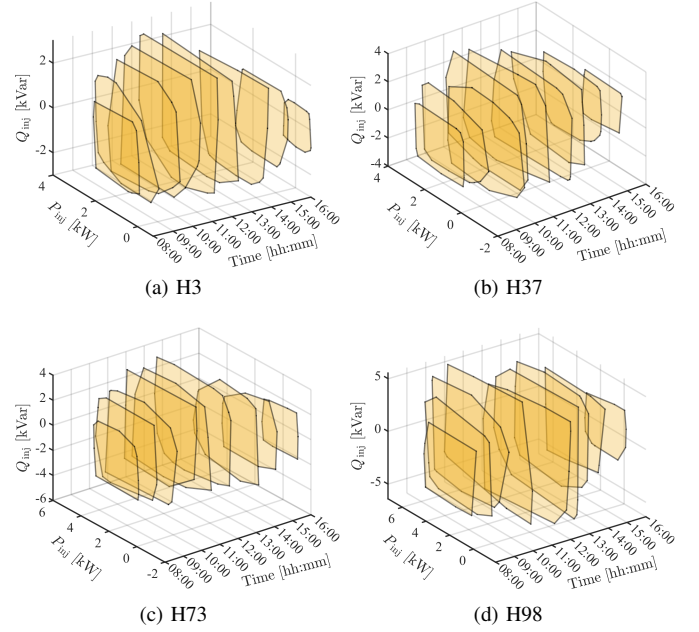
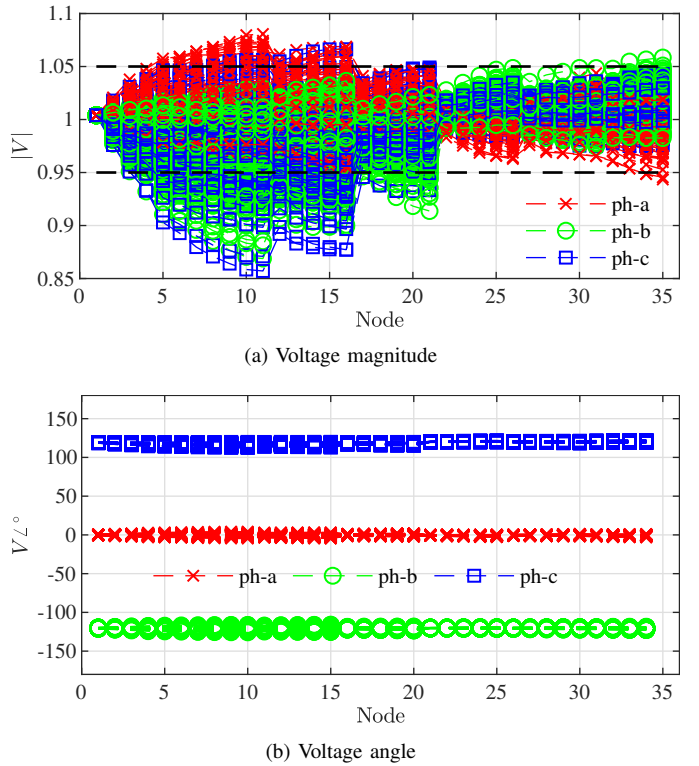
section II-B1. For this purpose, N_s is increased from 2 to 500 in steps of 1 and for each step, the value of β_{\max} is calculated. Fig. 5 shows the variation of β_{\max} with N_s . From the plot, the threshold is set to be 0.001 ($= 0.1\%$) and the corresponding value of N_s is obtained as 100. Also, it is observed that beyond $N_s = 100$, there is no significant improvement in the value of β_{\max} . Following this, $N_s = 100$ sampling instances in the LHS search space are considered and 100 three-phase load flow scenarios are performed to determine household DOEs at each time step.

A. The behaviour of household operating envelopes

Considering $N_s = 100$, the dynamic behaviour of OEs of 4 households equipped with different PV inverters (see Table II for details) is studied for a period of 24-hours. According to Fig. 6, operating envelopes tend to expand from 09:00 until around 12:00. Afterwards, the envelope shrinks from around 12:00 to 16:00. This can be understood by analysing the variation of the PV profile in Fig. 4. For instance, when the PV generation is low for all households (around 08:00 and 16:00), the envelope is small whereas when the PV generation is at the peak for all households (occurs around 12:00), the envelope remains large. For the rest of the period, i.e., from 09:00 to 12:00 and 12:00 to 16:00, the operating envelope of each household tends to follow its identical PV profile. On the other hand, the dynamic behaviour of operating envelopes provides implications to the flexibility at end-users' POC during different times of the day. When PV generation is low, a household will have significantly less or no flexibility whereas when PV generation is at its peak, the flexibility at the POC will be maximum. Moreover, the average execution time, i.e., the time to execute one step of the real-time algorithm in determining household DOEs, is approximately 25.36 sec ($\ll 5$ -min). Since this is compliant

TABLE II
DETAILS OF HOUSEHOLD UNDER STUDY

House #	Connected bus	PV rating [kWp]	electrical distance from bus ① [m]
3	②	4.0	40
37	⑭	5.0	301
73	⑳	6.0	200
98	㉔	8.0	211

Fig. 6. The behaviour of household time-varying envelopes under $N_s = 100$ (the variation from 08:00 to 16:00 is shown for clarity)Fig. 7. Voltage magnitude and angle at each node considering $N_s = 100$ at 12:00

with the market clearing interval [44], it can be claimed that the overall approach is scalable practically.

Fig. 7 shows voltage magnitudes and angles of each three-phase bus that is obtained by performing $N_s = 100$ load flow scenarios at 12:00. It can be clearly observed from Fig. 7a that voltage magnitudes differ in each phase of all buses,

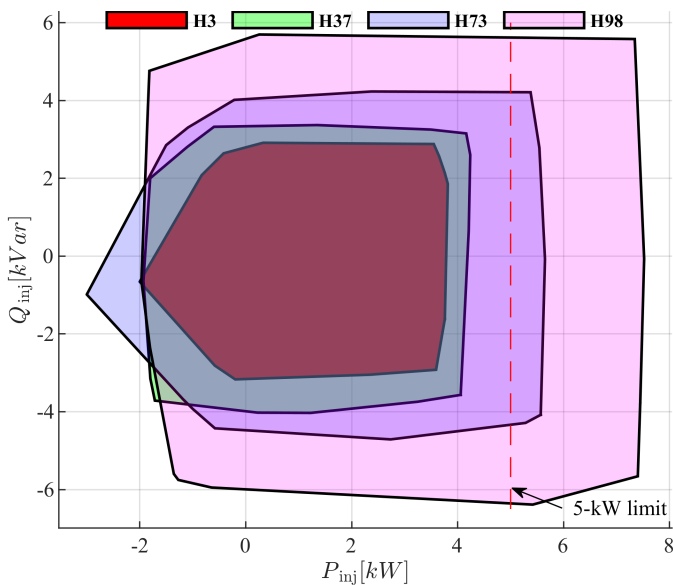


Fig. 8. Comparison of the overall feasible region of operation of households 3, 37, 73 and 98 throughout 24-hours

thus, leading to voltage unbalance. On the other hand, it is also noticed that for certain probabilistic load flow scenarios, P-Q injections obtained from the LHS search space of each POC results in the violation of voltage statutory limits given by $[0.95, 1.05]$ pu. Nonetheless, such scenarios are omitted in constructing household DOEs. Moving on to Fig. 7b, it is observed that phase voltage angles are nearly separated by 120° .

Fig. 8 depicts the overall FOR in the P-Q plane of households given in Table II throughout 24-hours (calculated as in section II-B3). It can be observed from the figure that, the overall feasible region is proportional to the size of the PV inverter. For instance, the overall envelope size is larger in household 98 (equipped with an 8.0 kWp inverter) compared to household 3 which is equipped with a 4.0 kWp inverter. On the other hand, it is also seen that, the overall feasible region is approximately asymmetric and tends to shift towards the region $P_{inj} > 0$ (exporting power) as the size of the PV inverter increases. In addition to that, the overall feasible region tends to stretch out along Q_{inj} axis as the inverter rating increases. This overall behaviour is intuitive as households are capable of exporting more active power to the grid if solar generation is available and the inverter rating is high. The reactive power limits introduced in (4) provide flexibility in both $Q_{inj} > 0$ and $Q_{inj} < 0$ directions. A further inspection of the results suggests that for households 73 and 98 equipped with 6.0 kWp and 8.0 kWp inverters respectively, operating envelopes allow active power exports beyond 5 kW fixed export limit [1]. Thus, the proposed approach for operating envelopes supports greater utilisation of existing household DER assets.

B. The behaviour of aggregate operating envelopes

The aggregate envelope of downstream nodes (node ②-③⑤ in Fig. 3) at each time instant is shown in Fig. 9. Similar to

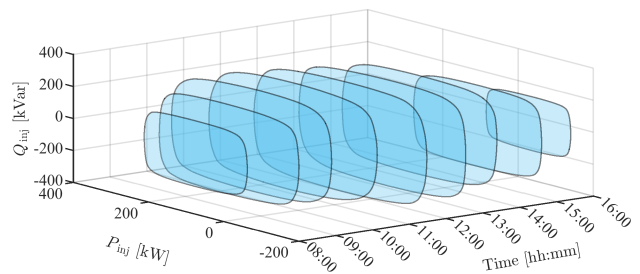


Fig. 9. The behaviour of aggregate time-varying operating envelopes (\mathcal{A}_t for $t \in \mathcal{T}$) at the LV distribution transformer ① (the variation from 08:00 to 16:00 is shown for clarity)

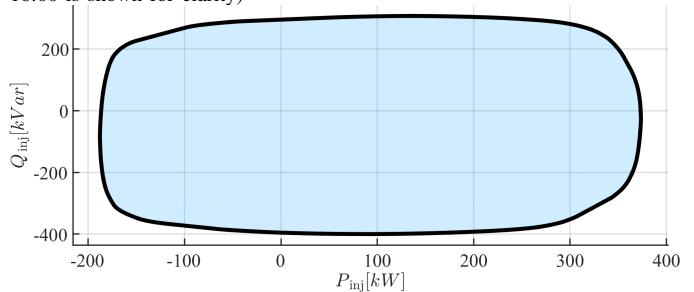


Fig. 10. The overall aggregate feasible region of operation (\mathcal{A}) of the LV distribution transformer ① over a period of 24-hours

household DOEs, the aggregate envelope expands as the solar generation increases and shrinks when the solar generation reduces. Also, compared to household DOEs, the boundaries of aggregate envelopes are smoother due to the *Minkowski* addition of individual envelopes as described in section II-B2. While time-varying aggregate envelopes are helpful for the DERA in assessing the flexibility of a particular feeder in real-time, it is also understood that the flexibility at node ① is an accumulation of individual flexibility provided by rooftop PV generation at each household.

Fig. 10 shows the overall feasible region of operation at node ① throughout 24-hours. As can be seen from the figure, the overall FOR obtains an outer approximation of aggregate time-varying operating envelopes and encapsulates the region $-200 \leq P_{inj} < 350$ kW and $-400 < Q_{inj} < 250$ kVar.

Fig. 11a illustrates the probability density of aggregate time-varying envelopes in the P-Q space over a period of 24 hours. Fig. 11b represents the probability density of region A which is bounded by $-165 \leq P_{inj} < -20$ kW and $-75 < Q_{inj} < 10$ kVar. It can be clearly seen from Fig. 11b that the P-Q feasible operating points are more likely to fall in the region $-80 \leq P_{inj} < -20$ kW and $-30 < Q_{inj} < 0$ kVar compared to the wider FOR of the overall aggregate envelope observed in Fig. 10. For instance, the region where the probability is high only corresponds to 0.50% of the total area of the overall aggregate feasible region. This is expected as the overall aggregate FOR represents an outer approximation of time-varying aggregate envelopes, not a probabilistic estimate. Nonetheless, with similar information on overall aggregate envelopes from multiple LV feeder networks, the DERA is able to assess the flexibility at each feeder and bid in day-ahead markets to maximise its social welfare while ensuring

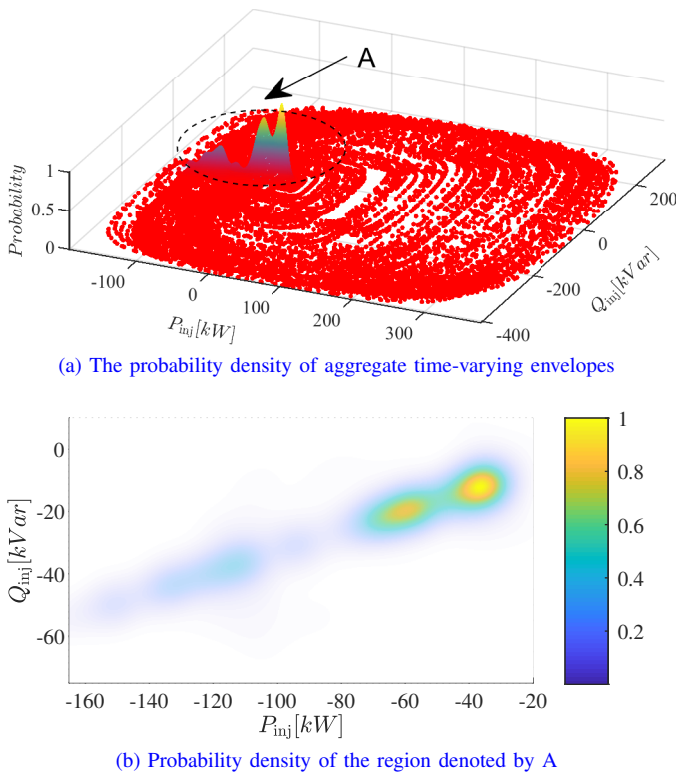


Fig. 11. The probability density of aggregate time-varying envelopes for 24-hours

secure network operation.

IV. CONCLUSION

In this study, a novel approach is proposed for the DNSP to determine operating envelopes that explicitly account for the feasible operating regions of households. Under the proposed approach, the DNSP employs load flow studies on a Latin hypercube sampling search space followed by a *convex hull* approximation to determine envelopes that outline the FOR in the P-Q plane without violating statutory voltage limits. Furthermore, the DNSP also determines: 1) a feeder-level aggregate envelope that represents the aggregate flexibility of downstream nodes of the network; 2) household-level and feeder-level time-invariant envelopes that encapsulate the overall FOR for the forward horizon. Some of the key findings of the study are as follows:

- The behaviour of household operating envelopes confirms that end-user flexibility is proportional to the availability of rooftop PV generation and the inverter rating.
- With inverter ratings greater than 5 kWp, for certain time periods of the day, the proposed DOE scheme is able to export active power beyond 5 kW static limit without breaching network constraints. This leads to effective utilisation of consumer-owned DERs in LV distribution networks.
- Based on the probabilistic assessment of aggregate time-varying envelopes, it can be concluded that the actual operation in the P-Q plane is limited to a smaller region (approximately 0.5% in area) compared to the analytical

calculation of the overall aggregate feasible operating region.

- Considering typical LV distribution networks, the proposed approach is able to determine household envelopes in less than the 5-mins. Hence, it can be concluded that the overall approach is scalable.

These findings are particularly relevant for future DNSPs to achieve greater network utilisation while ensuring network integrity, and for DERAs to unlock greater profitability in wholesale electricity markets.

In future work, the authors would like to improve the robustness of the proposed DOE framework against uncertainties associated with long-term forecasts of household load and generation, imperfections in the underlying bi-directional communication infrastructure between the end-user and the grid, and limited knowledge of the physical network, e.g., topology, conductors, equipment specifications and ratings. In addition to that, it would also be interesting to extend the capabilities of the proposed approach to address network voltage unbalance.

ACKNOWLEDGMENT

The authors would like to thank for the support given by the University of Queensland – Centre for Energy Innovation (UQ-CEDI) under the Advance Queensland grant (grant no: AQPTP01216-17RD1).

REFERENCES

- [1] ENERGEX Limited, "STNW3510: Dynamic Standard for Small IES Connections," https://www.ergon.com.au/_data/assets/pdf_file/0004/962779/STNW3510-Dynamic-Standard-for-Small-IES-Connections.pdf.
- [2] Dynamic Operating Envelopes Working Group, "Outcomes Report," March 2022. [Online]. Available: <https://arena.gov.au/assets/2022/03/dynamic-operating-envelope-working-group-outcomes-report.pdf>
- [3] L. Blackhall, "On the calculation and use of dynamic operating envelopes," The Australian National University, Tech. Rep., 2020. [Online]. Available: <https://arena.gov.au/assets/2020/09/on-the-calculation-and-use-of-dynamic-operating-envelopes.pdf>
- [4] M. Liu and L. Ochoa, "Project EDGE - Deliverable 1.1 "Operating Envelopes Calculation Architecture"," Tech. Rep. [Online]. Available: https://www.researchgate.net/publication/348176636_Deliverable_11_Operating_Envelopes_Calculation_Architecture
- [5] Liu, Michael and Ochoa, Luis(Nando), "Project EDGE - Deliverable 1.2 "High-level Assessment of Objective Functions"," Tech. Rep. [Online]. Available: https://www.researchgate.net/publication/348404040_Deliverable_12_High-level_Assessment_of_Objective_Functions
- [6] K. Petrou, M. Z. Liu, A. T. Procopiou, L. F. Ochoa, J. Theunissen, and J. Harding, "Operating envelopes for prosumers in LV networks: A weighted proportional fairness approach," in *IEEE PES Innovative Smart Grid Technologies Conference Europe*, vol. 2020-October, oct 2020, pp. 579–583.
- [7] K. Petrou, A. T. Procopiou, L. Gutierrez-Lagos, M. Z. Liu, L. F. Ochoa, T. Langstaff, and J. M. Theunissen, "Ensuring distribution network integrity using dynamic operating limits for prosumers," *IEEE Transactions on Smart Grid*, vol. 12, no. 5, pp. 3877–3888, Sep. 2021.
- [8] V. Pillitteri and T. Brewer, "Guidelines for Smart Grid Cybersecurity," 2014.
- [9] Y. Yi and G. Verbič, "Fair operating envelopes under uncertainty using chance constrained optimal power flow," *Electric Power Systems Research*, vol. 213, p. 108465.
- [10] A. Attarha, S. M. N. R.A., P. Scott, and S. Thiebaux, "Network-Secure Envelopes Enabling Reliable DER Bidding in Energy and Reserve Markets," *IEEE Transactions on Smart Grid*, p. 1, 2021.
- [11] Y. Zabihinia Gerdroodbari, M. Khorasany, and R. Razzaghi, "Dynamic pq operating envelopes for prosumers in distribution networks," *Applied Energy*, vol. 325, p. 119757.

- [12] B. Liu and J. H. Braslavsky, "Sensitivity and robustness issues of operating envelopes in unbalanced distribution networks," *IEEE Access*, vol. 10, pp. 92 789–92 798, 2022.
- [13] K. Christakou, D. C. Tomozei, M. Bahramipناه, J. Y. Le Boudec, and M. Paolone, "Primary voltage control in active distribution networks via broadcast signals: The case of distributed storage," *IEEE Transactions on Smart Grid*, vol. 5, no. 5, pp. 2314–2325, 2014.
- [14] V. Rigoni, D. Flynn, and A. Keane, "Coordinating Demand Response Aggregation with LV Network Operational Constraints," *IEEE Transactions on Power Systems*, vol. 36, no. 2, pp. 979–990, mar 2021.
- [15] M. Z. Liu, L. F. Ochoa, P. K. C. Wong, and J. Theunissen, "Using OPF-Based Operating Envelopes to Facilitate Residential DER Services," *IEEE Transactions on Smart Grid*, vol. 13, no. 6, pp. 4494–4504, nov 2022.
- [16] M. Z. Liu, L. N. Ochoa, S. Riaz, P. Mancarella, T. Ting, J. San, and J. Theunissen, "Grid and Market Services From the Edge: Using Operating Envelopes to Unlock Network-Aware Bottom-Up Flexibility," *IEEE Power and Energy Magazine*, vol. 19, no. 4, pp. 52–62, jul 2021.
- [17] J. Silva, J. Sumaili, R. J. Bessa, L. Seca, M. A. Matos, V. Miranda, M. Caujolle, B. Goncer, and M. Sebastian-Viana, "Estimating the Active and Reactive Power Flexibility Area at the TSO-DSO Interface," *IEEE Transactions on Power Systems*, vol. 33, no. 5, pp. 4741–4750, 2018.
- [18] S. Riaz and P. Mancarella, "Modelling and Characterisation of Flexibility from Distributed Energy Resources," *IEEE Transactions on Power Systems*, vol. 37, no. 1, pp. 38–50, 2022.
- [19] D. M. Gonzalez, J. Hachenberger, J. Hinker, F. Rewald, U. Hager, C. Rehtanz, and J. Myrzik, "Determination of the time-dependent flexibility of active distribution networks to control their tso-dso interconnection power flow," in *20th Power Systems Computation Conference, PSCC 2018*. IEEE, jun 2018, pp. 1–8.
- [20] L. Ageeva, M. Majidi, and D. Pozo, "Coordination Between TSOs AND DSOs: Flexibility Domain Identification," in *The 12th Mediterranean Conference on Power Generation, Transmission, Distribution and Energy Conversion (MEDPOWER 2020)*, vol. 2020, nov 2020, pp. 429–434.
- [21] Energy Networks Australia, "Open Energy Networks Project: Energy Networks Australia Position Paper." [Online]. Available: <https://www.energynetworks.com.au/resources/reports/2020-reports-and-publications/open-energy-networks-project-energy-networks-australia-position-paper/>
- [22] Australian Energy Market Operator (AEMO), "Project EDGE: Public Interim Report." [Online]. Available: <https://aemo.com.au/-/media/files/initiatives/der/2022/public-interim-report.pdf?la=en>
- [23] V. Rigoni, D. Flynn, and A. Keane, "Coordinating Demand Response Aggregation With LV Network Operational Constraints," *IEEE Transactions on Power Systems*, vol. 36, no. 2, pp. 979–990, mar 2021.
- [24] The Australian National University, "On the implementation and publishing of operating envelopes: evolve Project M5 Knowledge Sharing Report," <https://arena.gov.au/assets/2021/04/evolve-on-the-implementation-and-publishing-of-operating-envelopes.pdf>.
- [25] E. Dall'Anese, S. S. Guggilam, A. Simonetto, Y. C. Chen, and S. V. Dhople, "Optimal Regulation of Virtual Power Plants," *IEEE Transactions on Power Systems*, vol. 33, no. 2, pp. 1868–1881, mar 2018.
- [26] E. Vrettos and G. Andersson, "Combined Load Frequency Control and active distribution network management with Thermostatically Controlled Loads," in *2013 IEEE International Conference on Smart Grid Communications (SmartGridComm)*. IEEE, oct 2013, pp. 247–252.
- [27] D. Gebbran, S. Mhanna, Y. Ma, A. C. Chapman, and G. Verbič, "Fair coordination of distributed energy resources with Volt-Var control and PV curtailment," *Applied Energy*, vol. 286, p. 116546, 2021.
- [28] E. Dall'Anese, S. V. Dhople, and G. B. Giannakis, "Optimal dispatch of photovoltaic inverters in residential distribution systems," *IEEE Transactions on Sustainable Energy*, vol. 5, no. 2, pp. 487–497, apr 2014.
- [29] Standards Australia, "Grid connection of energy systems via inverters, Part 2: Inverter requirements," <https://www.standards.org.au/standards-catalogue/sa-snz/other/el-042/as-slash-nzs--4777-dot-2-colon-2020>.
- [30] Energex, "Home Energy Management Systems." [Online]. Available: <https://www.energex.com.au/home/control-your-energy/smarter-energy/home-energy-management-systems>
- [31] Australian Energy Market Operator (AEMO), "Distributed Energy Resource Register," <https://aemo.com.au/en/energy-systems/electricity/der-register>.
- [32] R. Preece and J. V. Milanović, "Efficient Estimation of the Probability of Small-Disturbance Instability of Large Uncertain Power Systems," *IEEE Transactions on Power Systems*, vol. 31, no. 2, pp. 1063–1072, mar 2016.
- [33] D. A. Contreras and K. Rudion, "Improved Assessment of the Flexibility Range of Distribution Grids Using Linear Optimization," in *2018 Power Systems Computation Conference (PSCC)*, jun 2018, pp. 1–7.
- [34] T. Milford and O. Krause, "Managing DER in Distribution Networks Using State Estimation & Dynamic Operating Envelopes," in *2021 IEEE PES Innovative Smart Grid Technologies - Asia (ISGT Asia)*, 2021, pp. 1–5.
- [35] W. G. C. Bandara, D. Almeida, R. I. Godaliyadda, M. P. Ekanayake, and J. Ekanayake, "A complete state estimation algorithm for a three-phase four-wire low voltage distribution system with high penetration of solar pv," *International Journal of Electrical Power & Energy Systems*, vol. 124, p. 106332, 2021. [Online]. Available: <https://www.sciencedirect.com/science/article/pii/S0142061519336518>
- [36] M. T. De Berg, M. Van Kreveld, M. Overmars, and O. Schwarzkopf, *Computational geometry: algorithms and applications*. Springer Science & Business Media, 2000.
- [37] M. Herceg, M. Kvasnica, C. Jones, and M. Morari, "Multi-Parametric Toolbox 3.0," in *Proc. of the European Control Conference*, Zürich, Switzerland, July 17–19 2013, pp. 502–510, <http://control.ee.ethz.ch/~mpt>.
- [38] T. R. Ricciardi, K. Petrou, J. F. Franco, and L. F. Ochoa, "Defining Customer Export Limits in PV-Rich Low Voltage Networks," *IEEE Transactions on Power Systems*, vol. 34, no. 1, pp. 87–97, jan 2019.
- [39] K. E. Antoniadou-Plytaria, I. N. Kouveliotis-Lysikatos, P. S. Georgilakis, and N. D. Hatzigiorgiou, "Distributed and Decentralized Voltage Control of Smart Distribution Networks: Models, Methods, and Future Research," *IEEE Transactions on Smart Grid*, vol. 8, no. 6, pp. 2999–3008, nov 2017.
- [40] L. Wang, R. Yan, and T. K. Saha, "Voltage regulation challenges with unbalanced PV integration in low voltage distribution systems and the corresponding solution," *Applied Energy*, vol. 256, p. 113927, 2019.
- [41] The University of Queensland, "Centre for Energy Data Innovation (CEDI)." [Online]. Available: <https://cedi.uqcloud.net>
- [42] SMA Solar Technology AG, "SUNNY BOY 3.0/3.6/4.0/5.0," <https://www.sma.de/fileadmin/content/global/specials/documents/falcon-installer/SB30-50-DEN1708-V22web.pdf>.
- [43] R. C. Dugan and T. E. McDermott, "An open source platform for collaborating on smart grid research," in *2011 IEEE Power and Energy Society General Meeting*, 2011, pp. 1–7.
- [44] Australian Energy Market Operator, "NEM data dashboard." [Online]. Available: <https://aemo.com.au/en/energy-systems/electricity/national-electricity-market-nem/data-nem/data-dashboard-nem>

Gayan Lankeshwara (S'15) received the B.Sc.Eng. (Hons.) and M.Sc.Eng. degrees in electrical and electronic engineering from the University of Peradeniya, Sri Lanka, in 2016 and 2021. He is currently pursuing the Ph.D. degree in electrical engineering at The University of Queensland, Brisbane, QLD, Australia. His research interests include demand response, grid integration of distributed energy resources, distributed control and optimisation.

Rahul Sharma (SM'17) received the Masters of Engineering Science and Ph.D. degrees in electrical engineering from the University of Melbourne, Melbourne, VIC, Australia. He is currently a Senior Lecturer with the School of Information Technology and Electrical Engineering, The University of Queensland, Australia. His research interests include control of grid connected inverters, demand management algorithms, and monitoring of large solar farms. He is the lead founder and technical lead of solar farm monitoring start-up Solaris AI.

Ruifeng Yan (S'09, M'12) received a B.Eng. degree in Automation from the University of Science and Technology, China, in 2004, an M.Eng. degree in Electrical Engineering from the Australian National University, Australia, in 2007, and a Ph.D. degree in Power and Energy Systems from the University of Queensland, Australia, in 2012. He is currently a Senior Lecturer at the School of Information Technology and Electrical Engineering, University of Queensland, Australia. His research interests include power system operations and analysis and renewable energy integration into power networks.

Tapan K. Saha (M'93, SM'97, F'19) received the B.Sc. degree in electrical and electronic engineering from the Bangladesh University of Engineering and Technology, Dhaka, in 1982, the M.Tech. degree in electrical engineering from the Indian Institute of Technology Delhi, in 1985, and the Ph.D. degree from the University of Queensland, Brisbane, QLD, Australia, in 1994, where he is currently a Professor of Electrical Engineering and the Leader of Power, Energy and Control Engineering Discipline with the School of Information Technology and Electrical Engineering. His research interests include condition monitoring of electrical assets, power systems, and renewable energy integration to the grid. He is a Fellow and Chartered Professional Engineer of the Institution of Engineers, Australia. He is a Registered Professional Engineer of the State of Queensland.

Jovica V. Milanović (M'95, SM'98, F'10) is a Professor of Electrical Power Engineering and Head of the Department of Electrical and Electronic Engineering at the University of Manchester, U.K., and Honorary Professor at the University of Queensland, Australia and Visiting Professor at the University of Novi Sad and the University of Belgrade, Serbia. Professor Milanovic is Foreign member of the Serbian Academy of Engineering Sciences, Distinguished IEEE PES Lecturer, member of the IEEE Fellows Committee and the Editor-in-Chief of IEEE Transactions on Power Systems.